

Supporting information

Gadolinium tagging for high-precision measurements of 6 nm distances in protein assemblies by EPR

Hiromasa Yagi,¹ Debamalya Banerjee,² Bim Graham,³ Thomas Huber,¹ Daniella Goldfarb,² Gottfried Otting¹

¹Research School of Chemistry, Australian National University, Canberra, ACT 0200, Australia

²Department of Chemical Physics, Weizmann Institute of Science, Rehovot, 76100, Israel

³Medicinal Chemistry and Drug Action, Monash Institute of Pharmaceutical Sciences, Parkville, VIC 3052, Australia

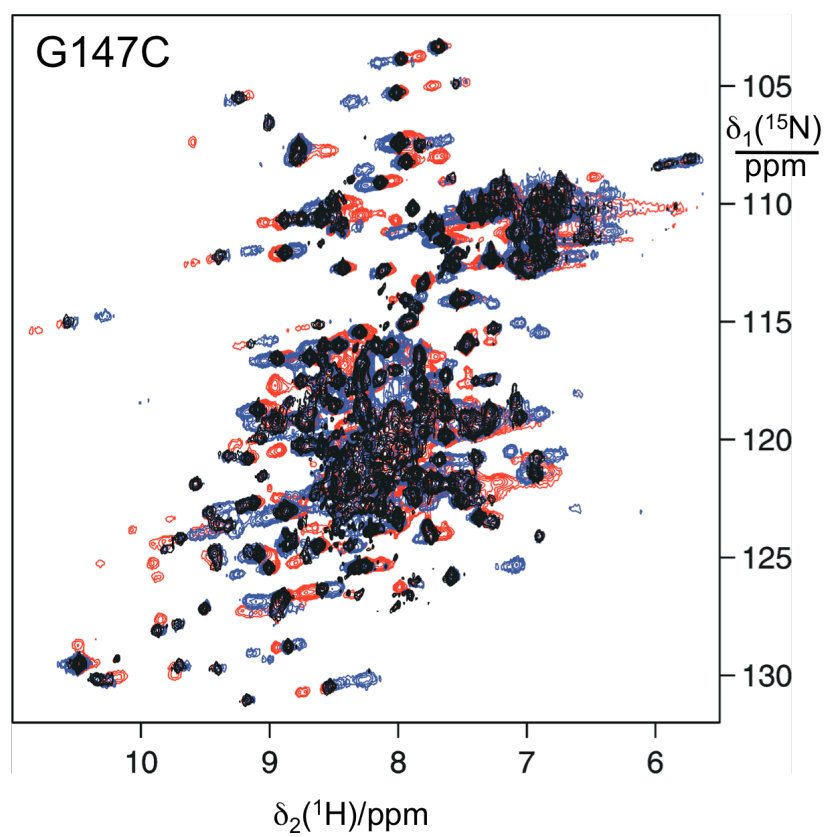
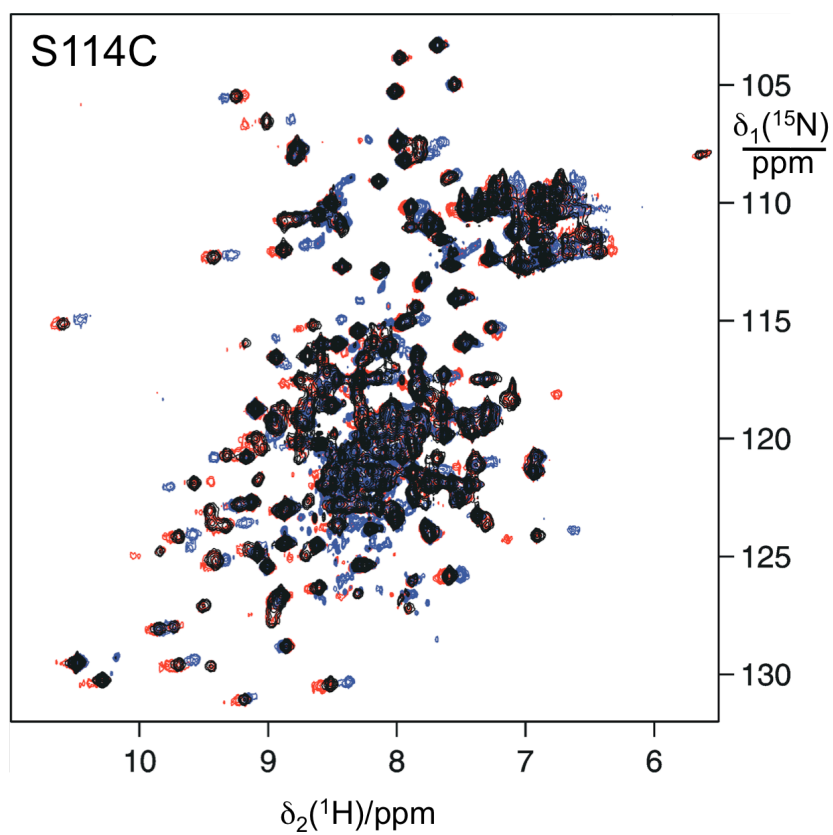
Sample preparation. The mutants S114C/C157S and G147C/C157S of ERp29 were cloned with a C-terminal His₆ tag into the expression plasmid pETMCSI (Neylon et al. 2000) for overproduction of the protein under control of the T7-promoter. Uniformly ¹⁵N-labeled samples of each ERp29 mutant were expressed in *E. coli* Rosetta (λ DE3)/pRARE cells. Cells were grown overnight in 5 mL of LB media and subsequently inoculated into 1 L of minimal media containing ¹⁵NH₄Cl as the sole nitrogen source at 37 °C. The protein expression was induced by adding 1 mM isopropyl β -D-1-thiogalactopyranoside (IPTG) at OD₆₀₀ of 0.6 and the cells were harvested 6 hours after IPTG induction. The perdeuterated protein was produced by growing the cells in minimal medium containing 90% D₂O. Selectively ¹⁵N-Lys labeled protein was obtained using the expression protocol for uniformly ¹⁵N-labeled protein except for adding 0.1 g/L ¹⁵N-Lys into minimal media containing ¹⁴NH₄Cl. In addition, a set of 5 combinatorially ¹⁵N-labeled samples of wild-type ERp29 was prepared by cell-free protein synthesis following the protocol described previously (Wu et al. 2006). All samples were purified as described previously (Liepinsh et al. 2001).

The ERp29 mutants were labeled with the C1 tag loaded with Gd³⁺ as follows. 0.1 mM protein solution in 50 mM Tris/HCl buffer, pH 7.6, was reduced with 5

equivalents of DTT and the DTT was washed out using a Millipore Ultra-4 centrifugal filter (molecular weight cut-off 10 kDa). The reduced protein solution was added slowly into a solution of 5 equivalents of C1 tag in the same buffer and kept at room temperature overnight. Excess tag was washed out with 20 mM MES buffer in D₂O, pH 4.9. Finally, the volume was reduced to about 80 μ L using centrifugal filters and deuterated glycerol was added to a final concentration of 20% (v/v) to reach a final protein concentration of 0.1 mM. For NMR measurements, protein samples were tagged in the same way using C1 tags loaded with Tb³⁺, Tm³⁺, and Y³⁺, except that the final buffer contained 90% H₂O/10% D₂O and no glycerol.

NMR measurements. NMR spectra were recorded using 0.3 mM solutions of the ERp29 mutants in 20 mM MES buffer, pH 4.9, at 31 °C on a Bruker Avance 800 MHz NMR spectrometer with a TCI cryoprobe. The backbone amide resonances were assigned by reference to the literature (Liepinsh et al. 2001) and using combinatorially labelled samples (Wu et al. 2006). PCSs were measured as the difference of the ¹H chemical shifts observed in the ¹⁵N-HSQC spectra of the ERp29 mutants labeled with the C1 tags loaded with paramagnetic ions (Tm³⁺ and Tb³⁺) minus the corresponding chemical shifts attached with the same tag loaded with diamagnetic ion (Y³⁺).

(A)



(B)

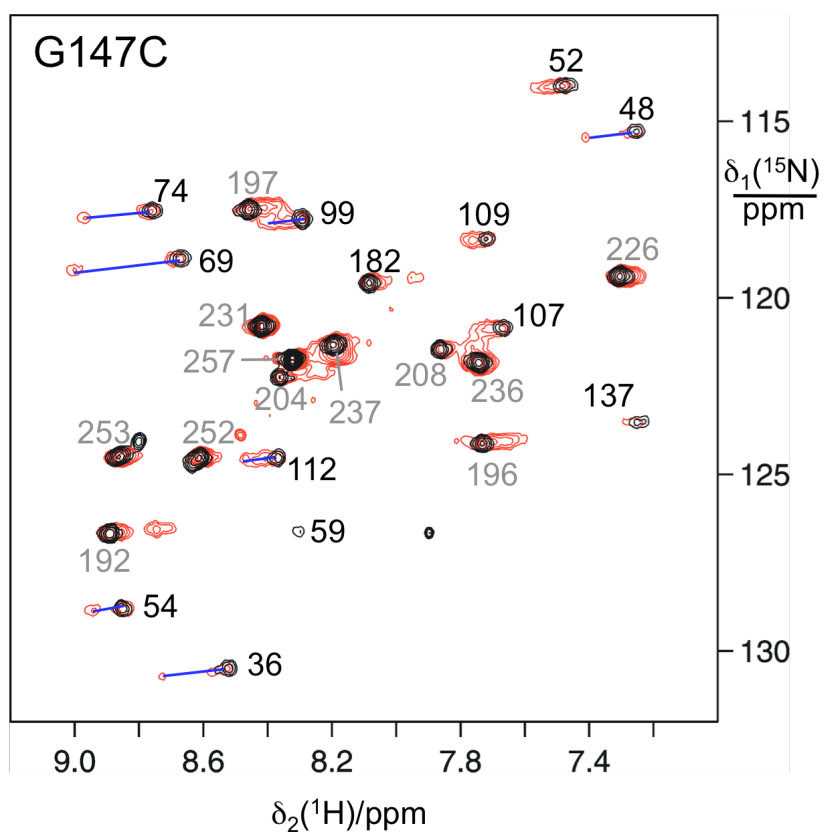
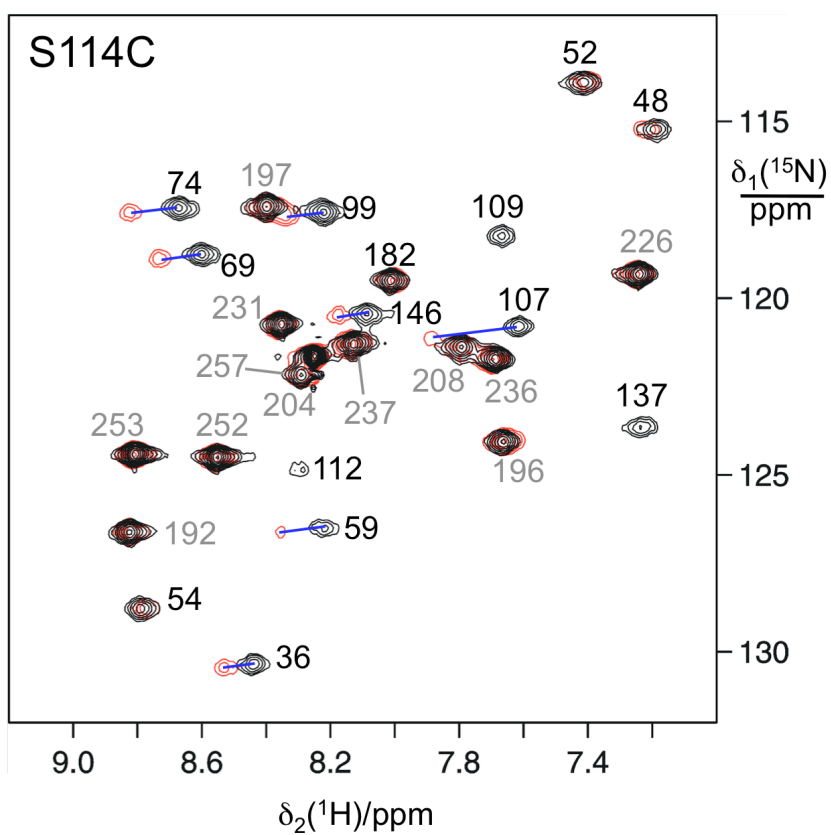


Figure S1 Superimposition of ^{15}N -HSQC spectra of 0.3 mM solutions of the mutants S114C and G147C ligated with C1 loaded with Y^{3+} (black peaks), Tb^{3+} (blue), or Tm^{3+} (red). All spectra were recorded at 31 °C on a Bruker 800 MHz NMR spectrometer in a 20 mM MES buffer, pH 4.9. (A) Samples prepared with uniform ^{15}N -labeling. (B) Samples prepared with selective ^{15}N -Lys labeling. The resonance assignments of the Lys residues in the N- and C-terminal domains are indicated in black and grey, respectively. Selected pairs of peaks from the samples containing Y^{3+} and Tm^{3+} tags are connected by blue lines to illustrate PCSs.

Table S1. PCSs of the backbone amide protons of different metal ions bound to the dimer of ERp29 S114C and G147C mutants tagged with C1.^[a]

residue	S114C		G147C	
	Tm ³⁺	Tb ³⁺	Tm ³⁺	Tb ³⁺
T35	0.09	-0.15		
K36	0.06	-0.14	0.20	-0.26
G37	0.04	-0.13	0.23	-0.28
T43		-0.17		
T45	0.03	-0.14	0.20	-0.25
F46	0.05	-0.12		
Y47		-0.08		-0.17
K48	0.04	-0.06	0.16	-0.19
I50				-0.09
K54	-0.02	0.03	0.09	-0.10
L57	0.06	-0.04		
K59	0.14			
Y64				-0.19
K69	0.14			
Q70			0.23	-0.27
K74	0.15		0.21	
A81	0.06	-0.08	0.41	-0.51
S82			0.41	-0.51
L86			0.37	-0.49
A89	0.09	-0.11		
G92	0.13	-0.22	0.12	-0.16
G97		-0.16	0.04	-0.11
D98	0.06	-0.15	0.13	-0.08
K99	0.12		0.08	
K107	0.28			
K109			0.04	
K112			0.10	
S114			0.10	-0.12
Y115				-0.16
F118			0.48	-0.56
Y119			0.31	
R122	-0.14	0.18		
D123	-0.07	0.09		
G124	-0.06	0.09	-0.07	0.10
N128			-0.17	
V130	-0.27	0.44		
V136			0.34	-0.40
K137		-0.44	0.53	-0.63
V138	0.20	-0.24	0.51	-0.56
G139	0.16	-0.21	0.59	-0.66
A140	0.23	-0.28		
Q148		0.01		

^aPCS values in ppm.

Table S2. $\Delta\chi$ tensors of different metal ions bound to the C1-tagged ERp29 mutant S114C, fitted using the crystallographic dimer or monomer structure.^a

Metal ion	$\Delta\chi_{ax}$ / 10^{-32} m^3	$\Delta\chi_{rh}$ / 10^{-32} m^3	Tensor axis	Coordinates of tensor axes		
dimer						
Tb ³⁺	11.9	3.8	x	-0.385	0.004	-0.923
	(11.4, 12.3)	(3.2, 4.3)	y	-0.898	0.229	0.376
			z	0.212	0.974	-0.084
Tm ³⁺	-8.1	-2.6	x	-0.604	0.026	-0.797
	(-8.9, -6.9)	(-3.4, -1.4)	y	-0.796	0.036	0.604
			z	0.044	0.999	-0.001
monomer						
Tb ³⁺	15.2	2.6	x	-0.257	0.052	-0.965
	(13.7, 16.3)	(1.0, 4.5)	y	-0.938	0.226	0.262
			z	0.231	0.973	-0.009
Tm ³⁺	-10.8	-2.7	x	-0.591	0.072	-0.803
	(-12.5, -9.4)	(-4.1, -1.5)	y	-0.800	0.075	0.595
			z	0.103	0.995	0.013

^[a] The tensors are listed in their unique representation (UTR; Schmitz et al. 2008) as obtained by fitting of the PCSs of Table S1 to ERp29 (PDB ID 2QC7; Barak et al. 2009) simultaneously using the PCSs induced by Tb³⁺ and Tm³⁺ and a common metal position. The covalent structure of the tag was taken into account as described in the main text. The orientations of the tensor axes are given as unit vectors with respect to the origin (0, 0, 0). Uncertainty ranges (shown in brackets) display the most extreme values identified among the family of 100 $\Delta\chi$ tensor optimizations using random subsets of 80% of the PCS data. The coordinates of the common metal position in the best fit were (20.531, 7.590, 22.013) for the dimer and (21.047, 7.078, 23.637) for the monomer structure.

Table S3. $\Delta\chi$ tensors of different metal ions bound to the C1-tagged ERp29 mutant G147C, fitted using the crystallographic dimer or monomer structure.^a

Metal ion	$\Delta\chi_{ax}$ / 10^{-32} m^3	$\Delta\chi_{rh}$ / 10^{-32} m^3	Tensor axis	Coordinates of tensor axes		
dimer						
Tb ³⁺	13.2	5.3	x	-0.389	0.679	0.623
	(12.4, 15.0)	(5.0, 5.8)	y	0.643	-0.283	0.711
			z	0.659	0.677	-0.327
Tm ³⁺	-8.8	-4.4	x	-0.360	0.639	0.680
	(-12.0, -8.5)	(-4.9, -4.0)	y	0.661	-0.340	0.669
			z	0.658	0.690	-0.300
monomer						
Tb ³⁺	15.3	6.1	x	-0.232	0.403	0.885
	(12.4, 19.6)	(4.8, 8.3)	y	0.733	-0.525	0.431
			z	0.639	0.749	-0.174
Tm ³⁺	-11.9	-4.9	x	-0.213	0.514	0.831
	(-13.6, -9.9)	(-6.6, -4.0)	y	0.706	-0.507	0.494
			z	0.675	0.692	-0.255

^a See footnote a in Table S2. The coordinates of the common metal position in the best fit were (27.763, -6.046, 7.628) for the dimer and (28.669, -8.515, 6.073) for the monomer structure.

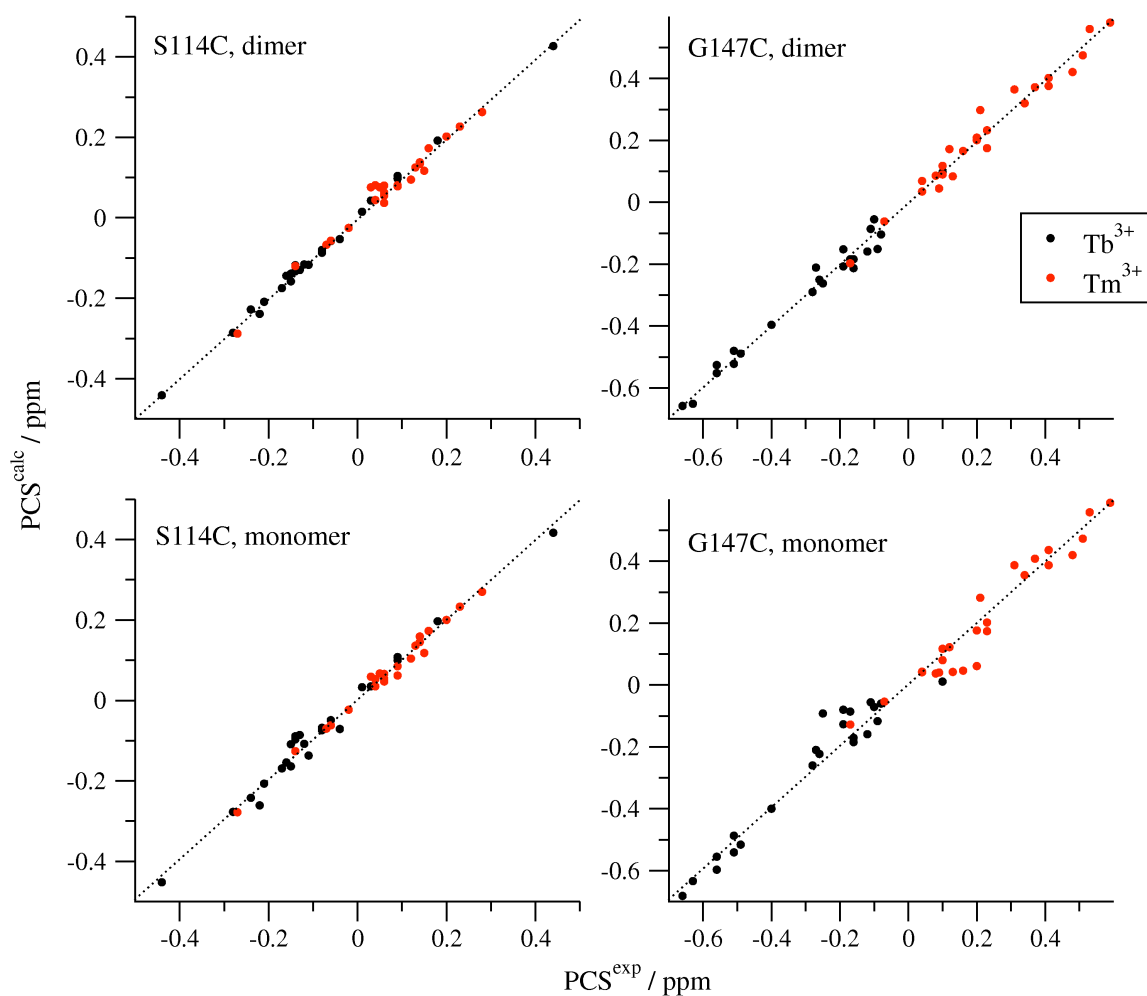


Figure S2 Plots of back-calculated versus experimental PCSs. The PCSs were fitted either to the monomer or the dimer of the crystal structure of human ERp29 (PDB ID 2QC7; Barak et al. 2009) as described in Table S2, using a common metal position for the data obtained with Tb^{3+} (black) and Tm^{3+} (red). In the case of the G147C mutant, the fits are better for the dimer than for the monomer. In the case of the S114C mutant, the difference is barely significant.

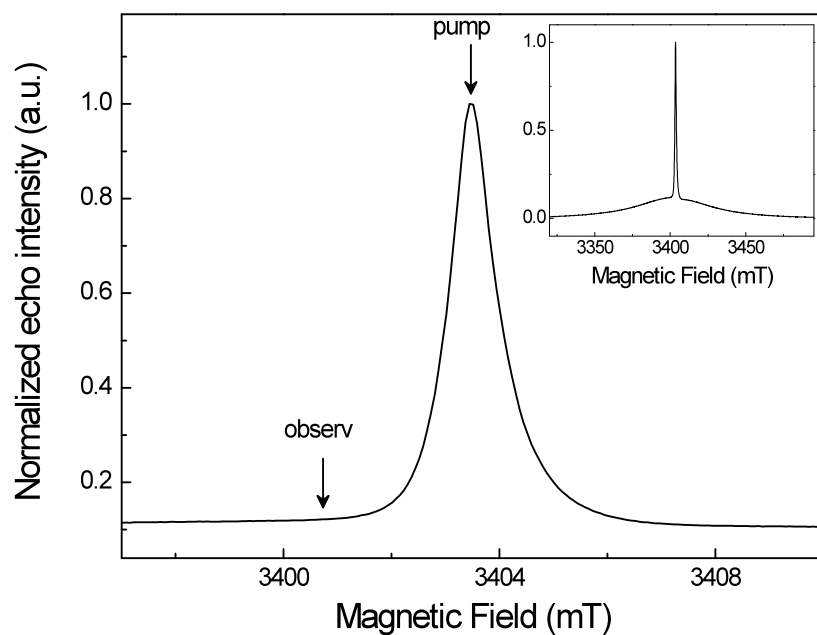


Figure S3 Echo-detected (ED) EPR spectrum around the central $|\frac{1}{2}\rangle \leftrightarrow |-\frac{1}{2}\rangle$ transition of the ERp29 mutant G147C recorded at 10 K. The measurements were carried out by a 2-pulse $\{\pi/2-\tau-\pi-\tau\}$ -echo sequence with $t(\pi/2) = 30$ ns, $t(\pi) = 60$ ns, and $\tau = 550$ ns. The positions of the pump and observe frequencies for the DEER experiment are indicated. The inset shows the full spectrum including the broad background from all other transitions in the $S = 7/2$ spin system. The ED-EPR spectrum of ERp29 S114C looked very similar.

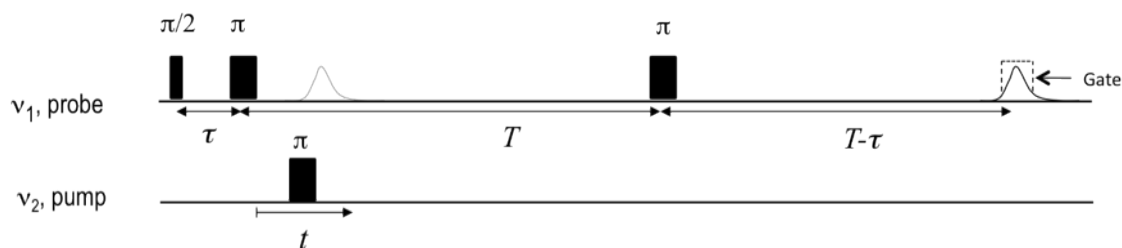


Figure S4 The four-pulse double electron-electron resonance (DEER) sequence used for the present work. A rectangular detection gate was placed on the refocused echo generated by the 2nd observe π pulse at time $2T$. The pump pulse was always set at the maximum of the echo intensity (see Figure S3) to engage a maximal number of spins in the experiment. Its frequency was set to the center of the cavity bandwidth. Observation pulse durations were (in the sequence of occurrence in the figure) 25, 50, and 50 ns. The pump pulse was 15 ns. The frequency separation $\Delta\nu$ between observation and pump pulses was 75 MHz. Sample preparation involved loading of about 3 μL of protein solution into a quartz capillary (0.6 mm I.D.) followed by rapid freezing and cooling to 10 K by insertion into a pre-cooled cryostat attached to the EPR magnet.

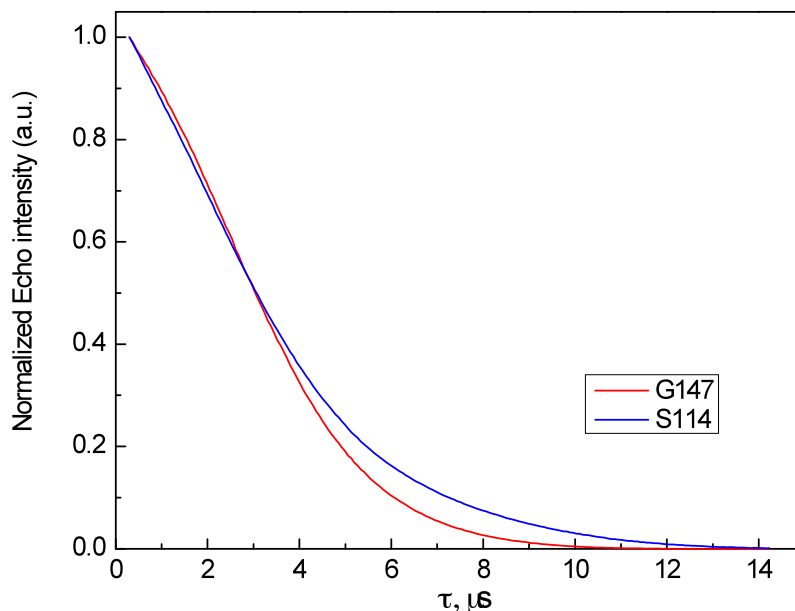
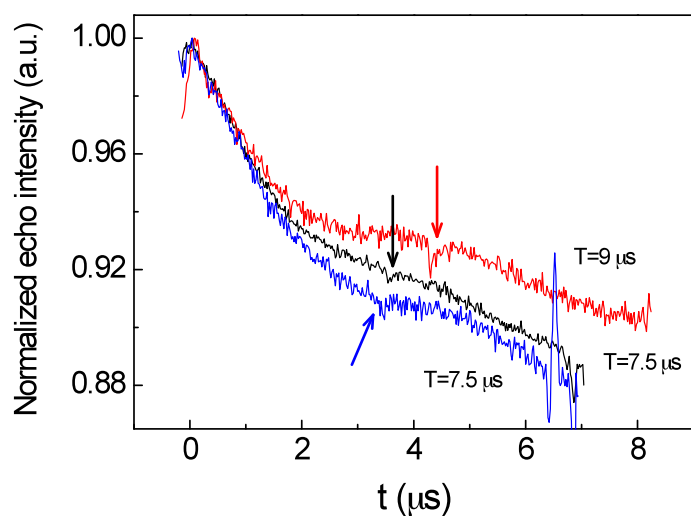


Figure S5 Decay of the echo intensity measured at the maximum of the ED-EPR spectrum at 10 K of ERp29 S114C (blue) and G147C (red). The measurements were carried out by a 2-pulse echo $\{\pi/2-\tau-\pi-\tau\}$ -echo sequence with pulse durations of 30 and 60 ns for the $\pi/2$ and π pulses, respectively, and the initial delay τ set to 300 ns. As the decays were non-exponential, the phase memory times T_M were estimated to be, respectively, 7.6 μs and 7.9 μs for the G147C and S114C mutants from the value of τ where the signal decayed to $1/e$ ($T_M = 2\tau_{1/e}$). Temperatures as low as 10 K were necessary to achieve the long phase memory times required for DEER measurements.

(A)



(B)

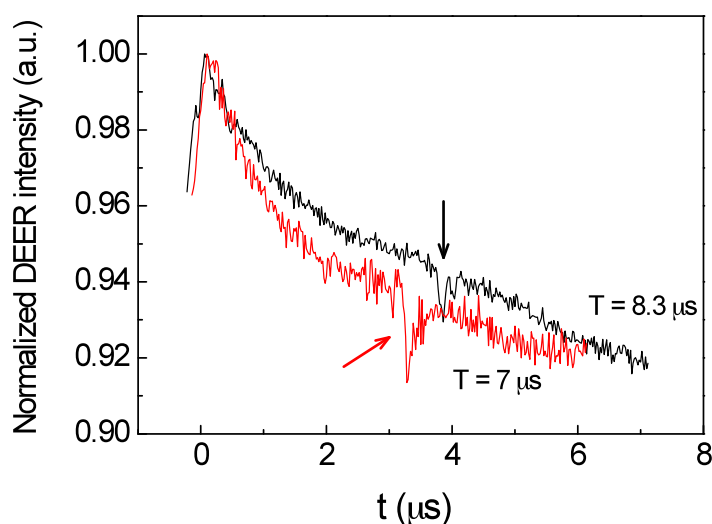


Figure S6 Normalized raw DEER traces (before background removal) recorded at 10 K with different parameters for (A) ERp29 S114C and (B) ERp29 G147C. The main differences between the traces are the T delays used. The traces were recorded using observe pulse durations of 25 and 50 ns for the $(\pi/2)_{\text{obs}}$ and $(\pi)_{\text{obs}}$ pulses, respectively, and a pump pulse $(\pi)_{\text{pump}}$ of 15 ns. The delay τ was set to 200 ns, except for the black trace in (a) which was recorded with $\tau = 300$ ns. The recovery delay between scans was 200 μs and the total recording time for a DEER trace was about 12 h. The irregular features identified by arrows at $t \approx T/2$ are experimental artifacts which probably arose from some spectral overlap between the pump and observe pulses and were not removed by phase cycling. These regions of the traces were manually replaced by interpolated data prior to analysis.

References

- Barak, N. N., Neumann, P., Sevvana, M., Schutkowski, M., Naumann, K., Malesevic, M., Reichart, H., Fischer, G., Stubbs, M. T., Ferrari, D. M. (2009) Crystal structure and functional analysis of the protein disulfide isomerase-related protein ERp29. *J. Mol. Biol.* **385**, 1630-1642.
- Liepinsh, E., Baryshev, M., Sharipo, A., Ingelman-Sundberg, M., Otting, G., Mkrtchian, S. (2001) Thioredoxin-fold as a homodimerization module in the putative chaperone ERp29: NMR structures of the domains and experimental model of the 51 kDa homodimer. *Structure* **9**, 457-471.
- Neylon, C., Brown, S. E., Kralicek, A. V., Miles, C. S., Love, C. A., Dixon, N. E. (2000) Interaction of the *Escherichia coli* replication terminator protein (Tus) with DNA: a model derived from DNA-binding studies of mutant proteins by surface plasmon resonance. *Biochemistry* **39**, 11989–11999.
- Schmitz, C., Stanton-Cook, M. J., Su, X.-C., Otting, G., Huber, T. (2008) Numbat: an interactive software tool for fitting $\Delta\chi$ -tensors to molecular coordinates using pseudocontact shifts. *J. Biomol. NMR* **41**, 179-189.
- Wu, P.S.C., Ozawa, K., Jergic, S., Su, X.-C., Dixon, N.E., Otting, G. (2006) Amino acid type identification in ^{15}N -HSQC spectra by combinatorial selective ^{15}N -labelling. *J. Biomol. NMR* **34**, 13-21.